Proceedings of the 28th IEEE
EMBS Annual International Conference
New York City, USA, Aug 30-Sept 3, 2006



# Vulnerability to electric shocks in the regionally-ischemic ventricles

Blanca Rodríguez, Brock Tice, Robert Blake, David Gavaghan and Natalia Trayanova, *Member, IEEE*

*Abstract*— **Although the majority of patients undergoing defibrillation suffer from coronary heart disease, little is known about defibrillation in the setting of ischemic disease. The goal of this study is to aid understanding of defibrillation failure in ischemic hearts by studying changes in cardiac vulnerability to electric shocks the first 10min following LAD occlusion. To do so, a 3D anatomically-accurate electrophysiologically-detailed bidomain model of the regionally ischemic ventricles following LAD occlusion was developed based on experimental data. The ventricles were paced at the apex and truncated exponential monophasic shocks were applied over a range of coupling intervals to determine the upper limit of vulnerability (ULV) and the vulnerable window (VW) in normoxia and 10min post-occlusion. Simulation results demonstrate that, despite the profound electrophysiological changes in the ischemic region, the ULV remains unchanged 10min post-occlusion because following high shock strengths ≥ULV virtual electrode polarization and postshock behavior remain unaffected by ischemia. However, the range of coupling intervals comprising the VW increases from spanning 60ms in normoxia to 90ms at 10min post-occlusion. The increased in vulnerability in regional ischemia stems from the fact that slow conduction and increased dispersion of refractoriness in the ischemic region increase the likelihood of the establishment of a reentrant circuit following shocks of strength <ULV.**

## I. Introduction

DEFIBRILLATION by timely application of a strong electric shock is the only effective therapy currently available to terminate lethal cardiac arrhythmias arising from ischemic injury. However, experimental studies have provided conflicting evidence on changes in defibrillation efficacy during ischemia. Some studies report an increase in defibrillation threshold (DFT) [1-4] while others find no change [5-7] or even a decrease in DFT [8].

Due to the strong link between the DFT and the upper limit of vulnerability (ULV), numerous studies have investigated the mechanisms of cardiac vulnerability to electric shocks in an attempt to understand defibrillation failure. However, the majority of these studies focused on healthy ventricles and rarely on hearts with ischemic disease, and thus little is known about the response of ischemic tissue to the application of electric shocks. This is in part due to the complexity and rapidity of ischemic changes, as well as to limitations in current experimental techniques.

Bidomain simulations have demonstrated ability to provide insight with high spatio-temporal resolution into the mechanisms of cardiac defibrillation in the healthy and the globally-ischemic ventricles.[9, 10] The present study extends this approach to cardiac vulnerability to electric shocks in regional ischemia. The goal is to aid understanding of defibrillation failure in ischemic hearts by studying changes in cardiac vulnerability to electric shocks in the first 10min following LAD occlusion.

## II. Methods

### A. Computational model

An anatomically-accurate electrophysiologically-detailed finite-element bidomain model of the rabbit ventricles was used [9-11]. Geometry and fiber orientation were based on anatomical data of the rabbit ventricles generated by McCulloch and Vetter [12]. Membrane kinetics were represented by a version of the Luo-Rudy dynamic model modified for defibrillation [13], which incorporates a formulation of the ATP-dependant $K^+$ current ($I_{KATP}$).[14]

Ischemic substrate at 10min post-occlusion was represented by changes in membrane dynamics due to hyperkalemia, acidosis, and hypoxia.[10] Specifically, to represent changes in ischemia-induced changes in membrane dynamics, extracellular $K^+$ concentration ($[K^+]_o$) was increased, whereas the maximum conductances of $Na^+$ and L-type $Ca^{2+}$ channels were decreased (by scaling factors $SF_{Na}$ and $SF_{CaL}$), representing inhibition by acidosis. Additionally, hypoxia-induced activation of $I_{K(ATP)}$ was considered by increasing the fraction of KATP channels opened ($p_{ATP}$).

Manuscript received April 3, 2006. This work was supported by the EPSRC-funded Integrative Biology e-Science pilot project (ref no: GR/S72023/01), by the UK National Grid Service, by the EU BioSim Grant (005137) and by AHA Established Investigator Award (N.T.), and the grant HL63195 from NIH (N.T).

B. R. is with University of Oxford (corresponding author: +44-1865-283557; fax: +44-1865-273839; e-mail: blanca@comlab.ox.ac.uk). D. G. is also with University of Oxford (e-mail: david.gavaghan@comlab.ox.ac.uk).

B. T., R. B. and N. T. are with Tulane University (e-mail: brock.tice@runbox.com, rblake@tulane.edu, nataliat@tulane.edu)

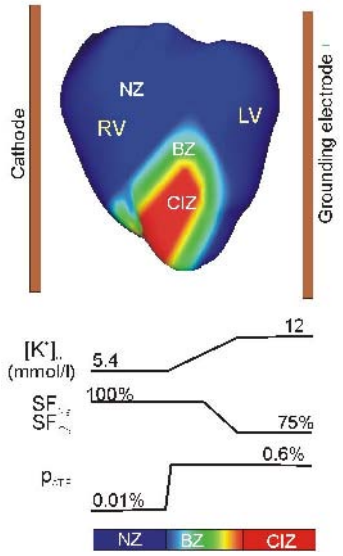


Figure 1. Anterior view of the regionally-ischemic ventricles with shock electrodes (top) and schematic illustrating variation of ischemic parameters in the normal zone (NZ), border zone (BZ) and central ischemic zone (CIZ) on the epicardium (bottom). LV= left ventricle, RV=right ventricle.

The region affected by lack of perfusion included 22.5% of total myocardial volume and was outlined based on experimental data (Fig. 1).[15] As shown in Fig. 1, the central ischemic region (CIZ) was surrounded by a border zone (BZ), which provided linear transition in ischemic parameters between the CIZ and the normal zone (NZ).[16] The model of regional ischemia also included ischemia-induced heterogeneities in the depth of the ventricular wall. The model considered an endocardial BZ [17], and transmural gradients in $[K^+]_o$ and $p_{ATP}$ between the epicardium and the subendocardium in the CIZ.[15, 18] Table 1 shows values of the ischemic parameters in the epicardium and the subendocardium of the CIZ.

### B. *Vulnerability to electric shocks*

The ventricles were paced at the apex at 250-ms basic cycle length. Following the seventh pacing stimulus, 8-ms long truncated exponential monophasic shocks of 65% tilt were applied via two planar electrodes in the perfusing chamber (Figure 1). The electrode next to the right ventricle (RV) was a cathode, and the electrode next to the left ventricle (LV) was a grounding electrode. Vulnerability grids were constructed in normoxia and regional ischemia by examining the outcome of shocks of various strengths applied at several coupling intervals (CIs) (measured from the onset of the last pacing stimulus). If the shock induced an arrhythmia of more than two extrabeats, the arrhythmia was classified as sustained.[9,10]

For normoxia and regional ischemia, ULV was determined as the lowest shock strength above which sustained reentry was no longer induced. The VW was determined as the interval between the shortest and the longest CIs for which sustained arrhythmia was induced. Increments in shock strength and CI used here were 1.5 V/cm and 10 ms, respectively. Finally, shock strengths referred to leading-edge value of the applied field.

TABLE 1
MODEL PARAMETERS

| | Normoxia | 10min post-occlusion epi | 10min post-occlusion endo |
|---|---|---|---|
| Extracellular $K^+$ concentration | 5.4mmol/L | 9mmol/L | 12mmol/L |
| Scaling factor for maximum conductance of $Na^+$ channels | 100% | 75% | 75% |
| Scaling factor for maximum conductance of $Ca^{2+}$ channels | 100% | 75% | 75% |
| Fraction of $I_{K(ATP)}$ channels activated | 0.01% | 0.6% | 0.36% |

## III. RESULTS AND DISCUSSION

### A. *Ischemia-induced electrophysiological changes*

As in previous studies, ischemia-induced alterations in membrane dynamics led to changes in action potential duration (APD) and resting potential ($V_{rest}$), resulting in changes in excitability and refractoriness. Table 2 shows values of APD and $V_{rest}$ for the ischemic conditions defined in Table 1. Note that, since regional ischemia leads to heterogeneous changes in membrane dynamics (as considered in the model and described in the Methods section), electrophysiological properties also vary within the CIZ and the BZ, leading to dispersion in refractoriness and conduction velocity in the regionally-ischemic ventricles.

TABLE 2
ELECTROPHYSIOLOGICAL PROPERTIES OF NORMAL AND ISCHEMIC TISSUE

| | Normoxia | 10min post-occlusion epi | 10min post-occlusion subendo |
|---|---|---|---|
| Action potential duration at 90% repolarization | 138ms | 69ms | 93ms |
| Resting potential | -85.4 | -75mV | -66mV |

### B. *Vulnerability to electric shocks in regional ischemia*

Results show that despite the profound electrophysiological changes induced by regional ischemia, the ULV remains at its normal value, 26.7V/cm, 10min following occlusion. However, the VW widens following LAD occlusion, spanning 60ms (CI from 110 to 170ms) in normoxia and 90ms (CI from 90 to 180ms) at 10min post-occlusion.

Fig. 2 depicts transmembrane potential distribution at the time of shock delivery (preshock panels), at shock end (0ms panel) and 5ms and 15ms after the end of a ULV strength shock applied at CI=130ms. CI=130ms is a CI at which the ULV occurs both in normoxia and regional ischemia, and thus it is the state more vulnerable to strong electric shocks. As shown in the preshock panels of Fig. 2, a larger amount of tissue is repolarized in ischemia than in normoxia at time of shock delivery, due to the decrease in repolarization times caused by APD shortening.[10] However, these differences in preshock state are overriden by the application of the

ULV strength shock and thus both epicardial and transmural virtual electrode polarization (VEP) are similar in normoxia and in regional ischemia (Fig. 2, 0ms panels). In both cases, the shock-end excitable area is mostly located within the septum and the LV free wall. Following shock end, wavefront propagation ensues, which very quickly engulfs the LV epicardial wall (Fig. 2, 5ms and 15ms panels). Whereas the whole epicardium is refractory soon after shock end, propagation continues within the LV free wall without a signature on the epicardium until it breaks through at 60ms postshock (Fig. 2, 60ms panel). Transmural views in Fig. 2 show that a reentrant circuit is established in the depth of the LV wall in both normoxia and regional ischemia (black arrows in transmural views of 100ms panels). As shown in Fig. 2, following the ULV strength shock, the reentrant circuit is established close to the base of the ventricles, and electrophysiological changes in the ischemic region, which is located close to the apex, do not interfere with it. Thus postshock activity and the outcome of the ULV strength shock are similar in normoxia and regional ischemia. This explains why the ULV remains in its normal value at 10min post-occlusion.

As stated above, simulation results show that, for shocks of strength <ULV, arrhythmias are induced at a wider range of CI in regional ischemia than in normoxia. Fig. 3 illustrates postshock electrical activity for a 22.8V/cm strength shock applied at CI=100ms in normoxia and regional ischemia. VEP at the end of the 22.8V/cm shock is similar in normoxia and regional ischemia, but differences in postshock electrical behavior between normoxia and regional ischemia develop that result in different outcomes of the shock. Application of a 22.8V/cm strength shock at CI=100ms results in sustained arrhythmia in regional ischemia but not in normoxia.

Following shock end, a wavefront propagates from apex to base through the midmyocardium of the LV free wall (Fig. 3, 20 and 50ms panels), breaking through the epicardium 71 and 87ms after shock end in regional ischemia and normoxia, respectively. Note that the site at which the wavefront breaks through following a 22.8V/cm shock (as in Fig. 3) is closer to the apex than following a stronger shock of 26.7V/cm strength (as in Fig. 2).

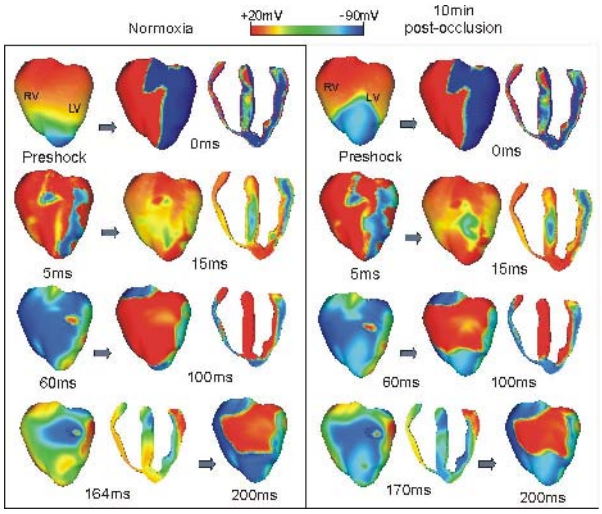


Fig. 2. Transmembrane potential distribution at time of shock delivery (preshock) and following a shock of 26.7V/cm strength applied at CI=130ms. Times refer to the end of the shock. Color scale is saturated, i.e., transmembrane potentials above 20mV and below –90mV appear red and blue, respectively.

As shown in Fig. 3A, in normoxia, once the wavefront breaks through the epicardium, propagation proceeds towards the septum and the RV (100ms panel), no unidirectional block of propagation occurs and the whole ventricles are refractory 140ms after shock end. Then propagation is blocked, no reentrant circuit is established (171 and 188ms panels), and the whole ventricular tissue is repolarized 188ms postshock.

In regional ischemia, the site at which the wavefront breaks through the epicardium following the 22.8V/cm shock is located within the lateral BZ of the ischemic region (arrow in 71ms panel, Fig. 3B). This determines the outcome of the shock. As shown in the 100 and 140 ms panels of Fig. 3B, after the breakthrough, propagation proceeds in all directions but becomes slower as it traverses the ischemic region due to ischemia-induced decrease in excitability. In addition, BZ tissue in the LV free wall recovers earlier than normal tissue due to decreased ERP caused by ischemia-induced APD shortening. Slow conduction in the IZ and short ERP in the BZ tissue favor the establishment of a reentrant circuit within the LV free wall, and thus a sustained arrhythmia is induced in the regionally-ischemic ventricles by the 22.8V/cm shock applied at CI=100ms (140, 171 and 188ms panels in Fig. 3B).

## IV. Conclusion

This study uses for the first time a sophisticated computer model of stimulation/defibrillation to provide mechanistic insight into the changes in cardiac vulnerability to electric shocks in the first 10min following LAD occlusion. Our results demonstrate that the ULV remains unchanged 10min post-occlusion, whereas the range of CIs comprising the VW widens in regional ischemia. The increased vulnerability in

regional ischemia stems from the fact that slow conduction and increased dispersion of refractoriness in the ischemic region increase the likelihood of the establishment of a reentrant circuit following shocks of strength <ULV.

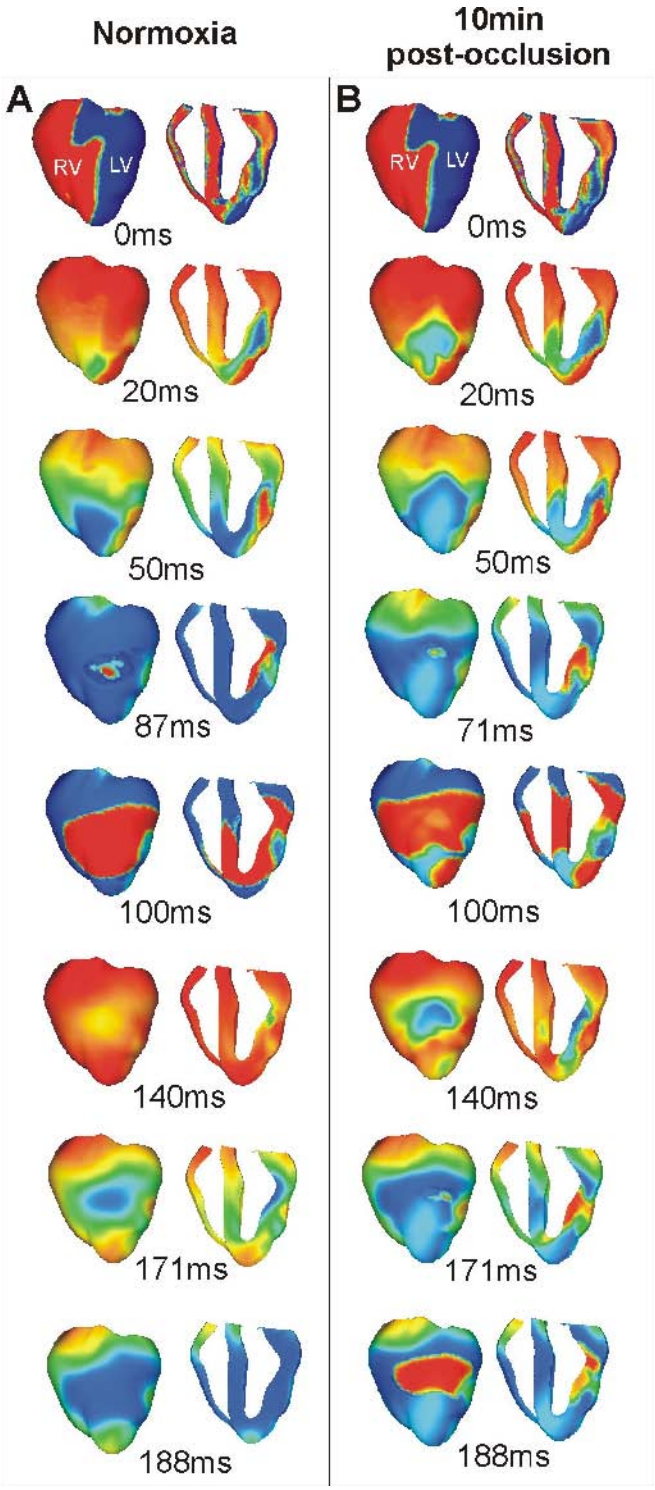


Fig. 3. Transmembrane potential distribution at time of shock delivery (preshock) and following a shock of 22.8V/cm strength applied at CI=100ms. Color scale as in Fig. 2.

## REFERENCES


[1] Babbs CF, Paris RL, Tacker WJ, and Bourland JD. Effects of myocardial infarction on catheter defibrillation threshold. Med Instrum 17: 18–20, 1983.

[2] Walcott GP, Killingsworth CR, Smith WM, and Ideker RE. Biphasic waveform external defibrillation threshold for spontaneous ventricular defibrillation secondary to acute ischemia. J Am Coll Cardiol 39: 359-365, 2002.

[3] Tacker WJ, Geddes LA, Cabler PS, and Moore AG. Electrical threshold for defibrillation of canine ventricles following myocardial infarction. Am J Physiol 88: 476–481, 1974.

[4] Qin H, Walcott GP, Killingsworth CR, Rollins DL, Smith WM, and Ideker RE. Impact of myocardial ischemia and reperfusion on ventricular defibrillation patterns, energy requirements, and detection of recovery. Circulation 105: 2537–2542, 2002.

[5] Jones DL, Sohla A, and Klein GJ. Internal cardiac defibrillation threshold: effects of acute ischemia. Pacing Clin Electrophysiol 9: 322–331, 1986.

[6] Kerber RE, Pandian NG, Hoyt R, Jensen SR, Koyanagi S, Graycel J, and Kieso R. Effect of ischemia, hypertrophy, hypoxia, acidosis and alkalosis on canine defibrillation. Am J Physiol Heart Circ Physiol 244: H825–H831, 1983.

[7] Ruffy R, Schwartz DJ, and Hieb BR. Influence of acute coronary artery occlusion on direct ventricular defibrillation in dogs. Med Instrum 14: 23–26, 1980.

[8] Arredondo MT, Armayor MR, and Valentinuzzi ME. Electrical defibrillation thresholds with transventricular simple-capacitor discharge under conditions of ischemia by acute coronary occlusion. *Med Prog Technol* 8: 175–181, 1982.

[9] Rodríguez B, Li L, Eason JC, Efimov IR, Trayanova NA. Differences between left and right ventricular chamber geometry affect cardiac vulnerability to electric shocks. *Circ Res*. 97:168-175, 2005.

[10] Rodríguez B, Tice BM, Eason JC, Aguel F, Trayanova N. Cardiac vulnerability to electric shocks during phase 1A of acute global ischemia. *Heart Rhythm*, 1(6):695-703, 2004.

[11] Trayanova NA, Eason JC, Aguel F. Computer simulations of cardiac defibrillation: A look inside the heart. *Comput Visual Sci.* 4:259-270, 2002.

[12] Vetter FJ, McCulloch AD. Three-dimensional analysis of regional cardiac function: a model of rabbit ventricular anatomy. *Prog Biophys Mol Biol*. 69:157–183, 1998.

[13] Ashihara T, Trayanova NA. Asymmetry in membrane responses to electric shocks: Insights from bidomain simulations. Biophysical Journal, 2004.

[14] Ferrero Jr JM, Saiz J, Ferrero JM, Thakor NV. Simulation of action potentials from metabolically impaired cardiac myocytes. Role of ATP-sensitive $K^+$ current. *Circ Res.* 79:208-221, 1996.

[15] Carmeliet E. 1999. Cardiac Ionic Currents and Acute Ischemia: From Channels to Arrhythmias. *Physiol Rev*. 79:917-1017.

[16] Ferrero JM Jr, Trenor B, Rodriguez B, Saiz J. 2003. Electrical activity and reentry during acute regional myocardial ischemia: insights from simulations. *Int J Bif Chaos.* 13:1-13.

[17] Wilkensky RL, Tranum-Jensen J, Coronel R, Wilde AAM, Fiolet JWT, Janse MJ. The subendocardial border zone during acute ischemia of the rabbit heart: an electrophysiologic, metabolic and morphologic correlative study. *Circulation.* 74: 1137-1146. 1986.

[18] Hill JL & Gettes LS. Effect of acute coronary artery occlusion on local myocardial extracellular $K^+$ activity in swine. *Circulation.* 61:768-778. 1980.